

# A Design of Autostereoscopic 3D Display Based on High PPI OLED Screen

Haoming Liu\*, Yiming Jia\*\*, Wentao Ying\*

\* Kunshan Visionox Technology Co., Ltd., Kunshan, China

\*\* Yungu (Gu'an) Technology Co., Ltd., Langfang, China

## Abstract

By compressing the effective emission area of OLED (Organic Light-Emitting Diode) pixels, it is possible to enhance the PPI (Pixels Per Inch) of the screen without increasing the risk of color mixing, thereby improving the resolution of autostereoscopic 3D displays. However, excessively large pixel pitches can lead to dark zones between viewpoints, which can impair the presentation of motion parallax. This paper proposes a design method for autostereoscopic 3D displays using OLED screens. By employing a large-angle oblique lenticular lens array and reducing the horizontal spacing between viewpoints, the width of the viewpoints generated by each subpixel is expanded, thereby eliminating dark zones between viewpoints and avoiding abrupt brightness changes. Based on this approach, a lenticular lens array with an oblique angle of  $78.3^\circ$  was attached to an 800-PPI OLED screen, achieving a field of view of  $\pm 25^\circ$  and delivering autostereoscopic 3D displays with good image depth and smooth motion parallax, which demonstrates the feasibility of the design.

## Author Keywords

OLED; autostereoscopic 3D display; high resolution; lenticular lens array.

## 1. Introduction

In the field of flat-panel displays, OLED has become the preferred choice for current mobile display devices due to its high contrast, wide color gamut, and flexible display forms [1, 2]. However, limited by the Fine Metal Mask (FMM) and the deposition process, the minimum subpixel pitch of conventional OLED screens is typically above approximately 20 micrometers. Additionally, the screen needs to maintain a certain aperture ratio. These two factors combined result in a relatively low pixel density of the screen, which in turn affects the screen resolution and limits its application in autostereoscopic 3D displays.

To address this shortcoming, we have compromised to a certain extent on the pixel aperture ratio, thereby achieving a higher PPI (Pixels Per Inch). This technology enhances the 3D display resolution and improves the 3D display effect of the OLED screen while maintaining the original OLED evaporation conditions. However, the reduction in the effective light-emitting area of the sub-pixels leads to a decrease in the width of the viewpoints generated by the sub-pixels through the lenses. When the sub-pixel aperture falls below a critical value, there is no overlap between viewpoints, causing an abrupt change in brightness as the human eye moves from one viewpoint to another, which affects the viewing experience.

Starting from fundamental design principles, this paper employs simulation methods to focus on discussing how to eliminate dark zones and improve display effects through the design of cylindrical lenses. Furthermore, we have attached the designed cylindrical lenses to an 800-PPI OLED screen, proving the correctness and feasibility of our design.

## 2. Design principle

Figure 1 showcases a high-PPI display panel with a pyramid-shaped pixel structure designed to enhance resolution. In this panel, each pixel consists of either a red-green pixel pair or a blue-green pixel pair. The number of green subpixels is double that of red or blue subpixels, with adjacent green subpixels sharing the same blue and red subpixels to achieve a wide color gamut display. Due to limitations in evaporation conditions, adjacent subpixels must maintain a certain spacing. The diameter of the apertures for red, green, and blue subpixels is set to be one-sixth of the minimum spacing between subpixels to minimize the size of each pixel unit and thereby increase pixel density. However, the reduction in light-emitting area also leads to a decrease in the projected area of the pixel after being magnified by the cylindrical lens, resulting in the emergence of dark zones.

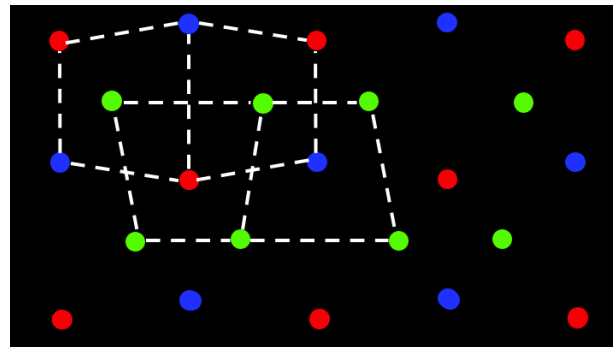
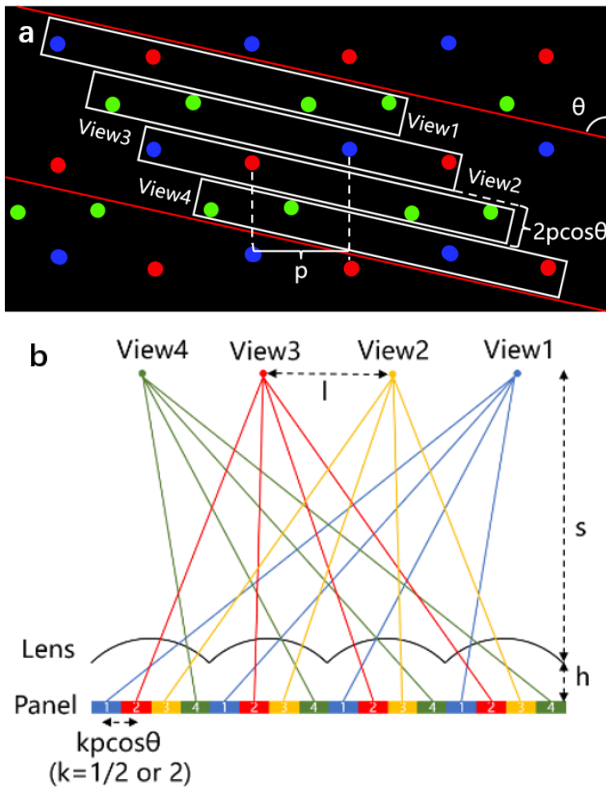


Figure 1. Pixel arrangement for high-PPI OLED screens.

Figure 2 depicts the relative positional relationship between the cylindrical lens array and the pixels. As shown in Figure 2(a), the red frame indicates the boundary of a single cylindrical lens, and the white frames represent the 3D pixels corresponding to different viewpoints (four viewpoints are illustrated for clarity). Since the red, green, and blue pixels corresponding to the same viewpoint are relatively close, while those corresponding to different viewpoints are spaced further apart, the pyramid-shaped pixel arrangement minimizes crosstalk between adjacent viewpoints while ensuring that the 3D image does not suffer from color deviation. This results in superior display performance compared to the conventional Pentile arrangement.

Given the tilt angle  $\theta$  of the lens, the horizontal pixel pitch  $p$ , the distance  $h$  between the pixels and the lenses, and the viewing distance  $s$ , the horizontal spacing  $l$  of the viewpoints can be expressed as:

$$l = \begin{cases} \frac{ps}{2h} & (0^\circ < \theta < 45^\circ) \\ \frac{2ps}{h} & (45^\circ < \theta < 90^\circ) \end{cases} \quad (1)$$



**Figure 2.** Diagram of cylindrical lens array and pixel arrangement: (a) Front view. (b) Side view.

The pixel pitch is fixed, and the viewing distance as well as the horizontal spacing of the viewpoints are determined at the initial stage of design. Therefore, when the tilt angle  $\theta$  increases beyond  $45^\circ$ , the distance  $h$  between the pixels and the lenses doubles from its initial value to maintain a constant horizontal spacing between the viewpoints. Since the screen is located at the focal plane of the lenses,  $h = f$ . The numerical aperture (NA) of the cylindrical lens can be expressed as:

$$NA = \frac{nD}{2f} \quad (2)$$

Where  $n$  is the refractive index of the lens material,  $D$  is the aperture of the lens, and  $f$  is the focal length of the lens. The relationship between the numerical aperture (NA) of the lens and the Airy disk produced by the lens can be expressed as:

$$r = \frac{0.61\lambda}{NA} \quad (3)$$

Where  $r$  is the distance from the position of maximum intensity at the center to the first dark pattern on the Airy disk, and  $\lambda$  is the wavelength of the light. By combining Equations (1), (2), and (3), it can be observed that as the tilt angle of the lens increases, the radius of the Airy disk increases, resulting in an increase in the width of a single viewpoint. Consequently, the size of the dark areas between the viewpoints is effectively controlled [3].

### 3. Simulation

To verify this conclusion, we set the observation distance to 30 cm, the viewpoint spacing to 6.5 cm (the average interpupillary distance of humans), and the number of viewpoints to 4. Using the non-sequential mode of ZEMAX, we simulated the light field distribution for structures with cylindrical lens tilt angles of  $\arctan(1/5)$  and  $\arctan(5)$ , respectively. The results are shown in Figure 3.

We set the ratio  $R$  of the peak half-width  $w$  of the two central viewpoints to the horizontal spacing  $l$  of the viewpoints as the evaluation criterion. A larger value of  $R$  indicates a smaller dark area. It can be found that as the tilt angle of the cylindrical lens increases, the value of  $R$  increases from the original 0.58 to 0.76, resulting in a certain degree of alleviation of the dark areas between the viewing angles.

According to Equation (1), the size of the dark area between viewpoints is also related to the set horizontal spacing between viewpoints. To obtain a smoother brightness distribution, under the condition of a cylindrical lens tilt angle of  $\arctan(5)$ , further simulations were conducted for cases where the spacing between adjacent viewpoints was 6.5/2 cm and 6.5/3 cm. The simulation results are shown in Figure 4.

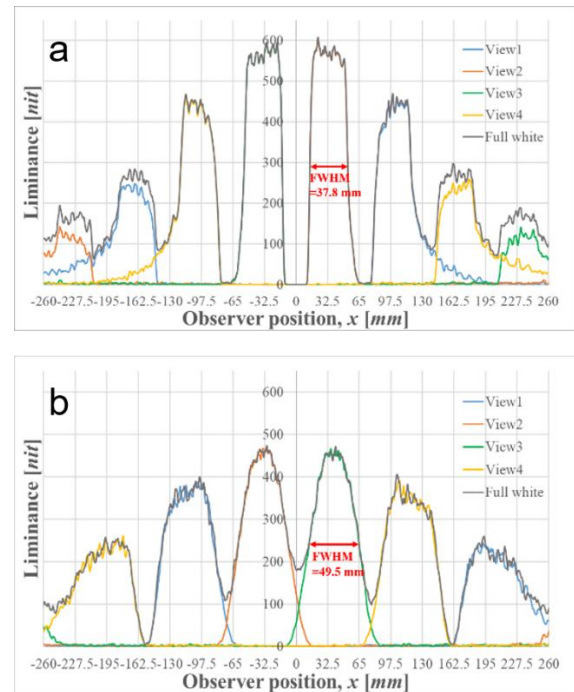


**Figure 3.** Light field distribution of lenticular lens at different tilt angles  $\theta$ : (a)  $\arctan(1/5)$ . (b)  $\arctan(5)$ .

Comparing the situation in Figure 3 with a horizontal spacing of 6.5 cm, it can be observed that as the set viewpoint spacing decreases, the  $R$  value gradually increases to 0.76, 0.79, and 0.87, respectively. In summary, under the premise of four viewpoints, with a tilt angle of  $\arctan(5)^\circ$  and a horizontal spacing between viewpoints of 6.5/3 cm, the optimal design result is achieved. Considering that the minimum brightness that the human eye can distinguish in a bright environment is around 400 nits, under the above conditions, the corresponding horizontal viewing distance  $x$  ranges from  $\pm 140$  mm, which translates to a field of view of  $\pm 25^\circ$ .

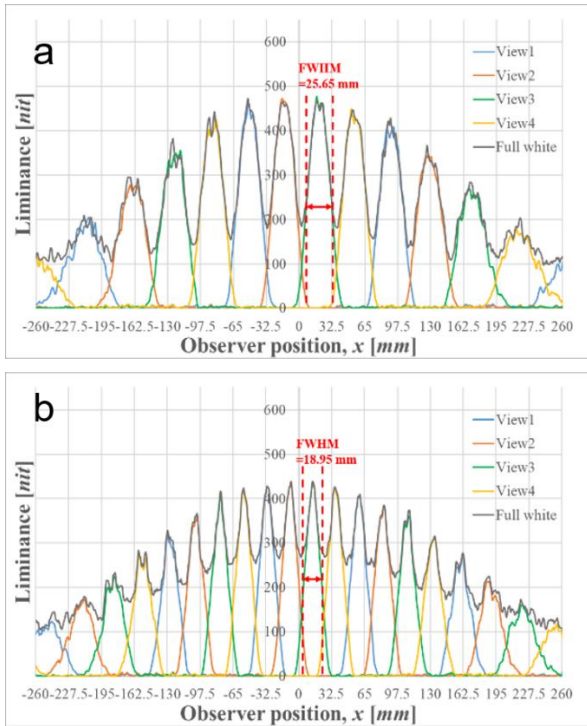


**Figure 4.** Light field distributions of different distances between adjacent views: (a) 6.5/2 cm; (b) 6.5/3 cm.

**4. Results and discussion**

To evaluate the proposed design method, we applied it to a 3.4-inch screen with an 800 ppi diamond-shaped pixel arrangement. The detailed parameters of the screen are shown in Table 1.

**Table 1.** Parameters of the autostereoscopic 3D display.

Name	Value
Screen size	3.4 inch
Resolution	2268*1476
Lens pitch	49.8 $\mu$ m
Slant angle	78.7° (arctan(5))
Optimal viewing distance	300 mm
Field of view	$\pm 25^\circ$

Figure 5 shows the white and black images corresponding to each eye within the four-viewpoint area at the center. Each 3D image is well separated according to each viewpoint, with no obvious crosstalk stripes appearing. In this test, the green images are used for the first and second viewing positions, while the red images are used for the third and fourth viewing positions.

To practically verify the 3D performance of the designed display, we combined and displayed two different dice images, aiming to

provide two distinct images based on the viewing position. Figures 6(a) and 6(b) show the images observed at the first and second, and third and fourth viewing positions, respectively. As shown in the figures, each image is well separated according to the perspective position. As the viewing position moves, there is no abrupt change in brightness.

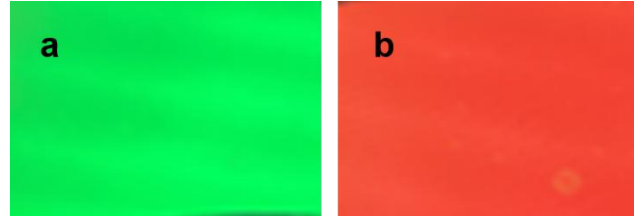


**Figure 5.** Images captured at the optimal viewing positions for green and red viewpoints: (a) First and second viewing positions; (b) Third and fourth viewing positions.

**5. Conclusions**

This paper proposes a design method for glasses-free 3D displays for high-PPI OLED screens, analyzing the factors that influence the size of the dark area between viewpoints. By employing a large-angle tilted cylindrical lens array and adjusting the set viewpoint spacing, the size of the dark area between viewpoints is effectively reduced. Based on the proposed design principles, a glasses-free 3D display with a 50° field of view is achieved using an 800 PPI screen with a diamond-shaped pixel arrangement. It is demonstrated to exhibit excellent viewpoint separation and smooth motion parallax effects.

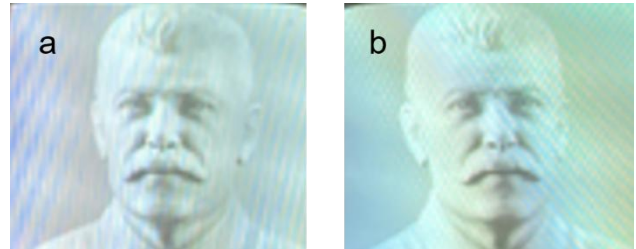


**Figure 6.** Disparity images captured at the optimal viewing position: (a) Left eye. (b) Right eye.

**6. References**

1. Song J, Lee H, Jeong E G, et al. Organic light - emitting diodes: pushing toward the limits and beyond[J]. *Advanced Materials*, 2020, 32(35): 1907539.
2. Huang Y, Hsiang E L, Deng M Y, et al. Mini-LED, Micro-LED and OLED displays: present status and future perspectives[J]. *Light: Science & Applications*, 2020, 9(1): 105.
3. Sim J H, Kim J, Kim C, et al. Novel biconvex structure electrowetting liquid lenticular lens for 2D/3D convertible display[J]. *Scientific Reports*, 2018, 8(1): 154.